Published in final edited form as:
Brain Res. 2014 January 13; 1542: 85–92. doi:10.1016/j.brainres.2013.10.031.

PROLYL CARBOXYPEPTIDASE mRNA EXPRESSION IN THE MOUSE BRAIN

Jin Kwon Jeong[1,2] and **Sabrina Diano**[1,2,3,4]

[1]Program in Integrative Cell Signaling and Neurobiology of Metabolism, New Haven, CT, USA

[2]Department of Ob/Gyn & Reproductive Sciences, New Haven, CT, USA

[3]Department of Neurobiology, New Haven, CT, USA

[4]Department of Comparative Medicine Yale University School of Medicine, New Haven, CT, USA

Abstract

Prolyl carboxypeptidase (PRCP), a serine protease, is widely expressed in the body including liver, lung, kidney and brain, with a variety of known substrates such as plasma prekallikrein, bradykinin, angiotensins II and III, and -MSH, suggesting its role in the processing of tissue-specific substrates. In the brain, PRCP has been shown to inactivate hypothalamic -MSH, thus modulating melanocortin signaling in the control of energy metabolism. While its expression pattern has been reported in the hypothalamus, little is known on the distribution of PRCP throughout the mouse brain. This study was undertaken to determine PRCP expression in the mouse brain. Radioactive in situ hybridization was performed to determine endogenous PRCP mRNA expression. In addition, using a gene-trap mouse model for PRCP deletion, X-gal staining was performed to further determine PRCP distribution. Results from both approaches showed that *PRCP* gene is broadly expressed in the brain.

Keywords

Prolyl carboxypeptidase; brain; distribution

1. Introduction

Prolyl carboxypeptidase (PRCP) is an enzyme of the carboxypeptidase (CPs) family which contains a serine residue in the active center, essential for catalytic activity (Abeywickrema et al., 2010; Soisson et al., 2010). PRCP cleaves only short peptides with a penultimate proline residue (Kumamoto et al., 1981).

PRCP was discovered over 40 years ago from studies of bradykinin metabolism in kidney (Yang et al., 1968). Since angiotensin II has the same C-terminus of bradykinin, the enzyme

Address all correspondence and requests for reprints to: Sabrina Diano, PhD Dept Ob/Gyn & Reproductive Sciences Yale University School of Medicine PO Box 208063 New Haven, CT 06520-208063 Ph: 203 7371216 Fax: 203 7854713 sabrina.diano@yale.edu.

Disclosure summary: The authors have nothing to disclose.

was named angiotensinase C. However, when its ability to cleave a variety of Pro-X bonds was shown, it was renamed PRCP.

PRCP (Yang et al., 1968; 1970) is a single chain protein of approximately 58 KDa. The C-terminal sequence contains an interesting “serine repeat” in which Ser is repeated as the 26th residue 6 out of 9 times (Tan et al., 1993). When the Ser residues are aligned to yield 26 residue repeats, the positions of some of the other residues also fall into a pattern. The significance of this repeat region is not clear, but it might be involved in the maintenance of a secondary or tertiary structural motif or in the formation of the homodimer. The gene encoding human PRCP is on chromosome 11, while in the mouse it is on chromosome 7.

PRCP has an acidic pH optima (=5.0) when hydrolyzing short synthetic peptide substrates (Odya et al 1978; Jackman et al., 1990; Tan et al., 1993), but it has been found that it retains significant activity at neutral pH range. Indeed, at a physiological pH, α-melanocyte stimulating hormone (α-MSH) is a better substrate for PRCP than angiotensin II (Wallingford et al., 2009).

PRCP activity has been detected in a variety of cells and organs both in rodents and human (Kumamoto et al., 1981; Skidgel et al., 1981; Tan et al., 1993). Within the cell, it has been localized in lysosomes (Kumamoto et al., 1981; Skidgel et al., 1981; Jackman et al., 1995). However, it has also been found to be released in response to stimulation appearing in extracellular media or biological fluids (Yang et al., 1960; Miller et al., 1991). In mice, like humans, PRCP is expressed in peripheral tissues such as kidney, liver, heart and spleen. In addition, PRCP is also expressed in the Central Nervous System (CNS; Wallingford et al., 2009). Specifically, within the CNS, recent studies have shown PRCP expression and regulation in the hypothalamus (Wallingford et al., 2009; Jeong et al., 2012a, b, 2013).

The distribution pattern of PRCP in the CNS has not been explored in details. Thus, our study was undertaken to determine the expression pattern of PRCP within the CNS.

2. RESULTS

Radioactive in situ hybridization using a riboprobe specific to PRCP mRNA was performed in adult C57Bl6 mouse brains (Fig 1). In addition, PRCP expression pattern was studied using X-gal staining in PRCP transgenic mice in which trapped PRCP gene contained an insertion that had the following regions in its vector (pGT1TM) from 5’ to 3’ called SA (splice acceptor), CD4-TM, and a lacZ reporter (Skarnes et al., 1995; Wallingford et al., 2009; Figs 2 and 3). The results obtained from both methodologies were overlapping. PRCP gene expression was observed throughout the mouse brain with a differential expression pattern (Table 1).

2.1 Expression of PRCP in the telencephalon

The overall localization and expression levels of PRCP mRNA in adult mice brain is summarized in Table 1.

The greatest levels of both endogenous and transgene signals were detected in the cerebral cortex with very strong labeling in the cingulate (Cing Ctx; Fig. 1C,F,O, Fig. 2A-F, Fig. 3A) and piriform cortex (Pir ctx; Fig. 1B,F,Q, Fig.2A-F, Fig. 3C). Other areas of the cortex showed moderate signal intensity. Within the limbic system, strong signal was detected in the hippocampus and in the amygdaloid complex. Both X-gal and silver grain density were weaker in the rostral portion of the hippocampus but became stronger in the caudal portion. Within the hippocampus, both signals were strong in all regions of the Ammon's horn and in the dentate gyrus (Fig. 1B,C,F,G,P, Fig.2C-F, Fig.3B). In the amygdala, high intensity of the

signal was detected within the the basolateral- (Fig. 1F,N, Fig. 2D and Fig. 3C) and central-amygdaloid nucleus, while moderate signals were observed in the anterior-amygdaloid nucleus (BLA; Fig.2D and Fig. 3C). PRCP labeling was also detected within the septum pellucidum, specifically the lateral septal nucleus (LSN; Fig. 2A).

2.2 Expression of PRCP in the diencephalon

Strong PRCP expression was detected within the thalamus. Specifically, the paraventricular thalamic nucleus (PV; Fig. 1F, Fig. 2B-D, Fig. 3G) and the Xiphoid thalamic nucleus (Xi; Fig. 2C) showed the stronger staining within the thalamic formation.

In the epithalanus, the habenular nucleus (MHb) showed significant staining (Fig. 2D, Fig. 3H). Within the hypothalamus, moderate to weak levels of both endogenous PRCP mRNA and X-gal staining were detected. Specifically, both X-gal staining and in situ hybridization for PRCP mRNA show moderate signals in the medial (MPO) and lateral preoptic area (LPO; Fig. 1I, Fig.2A and fig. 3D), in the paraventricular nucleus (PVN; Fig. 1B, J; Fig 2C and Fig. 3F), in the supraoptic nucleus (SO; Fig. 2B-C and Fig. 3E), in the dorsomedial hypothalamic area (DMH; Fig. 1C,K, Fig. 2D and Fig. 3J), in the lateral hypothalamus (LH; Fig. 1F,L, Fig. 2D and Fig. 3I,J) and in the arcuate nucleus (ARC; Fig. 1C,K, Fig. 2D and Fig. 3I). On the other hand, while by in situ hybridization, moderate signals for PRCP mRNA expression was detected in the ventromedial hypothalamus (VMH; Fig. 1C,K), a very weak and/or inconsistent staining by X-gal staining was detected (Fig. 2D and Fig. 3I). Similar discrepancy was found in the bed nucleus of stria terminalis (BST), in which only hybridization signal was detectable, but not X-gal staining (data not shown).

2.3 PRCP expression in the mesencephalon and rhombencephalon

In the midbrain, PRCP labeling was detected in the zona incerta (ZI; Fig. 2E) and the ventral tegmental area (VTA; Fig. 1M, Fig. 2F, Fig. 3K).

Within the pons, several pontine nucleis showed strong PRCP signal including the pontine reticular nucleus (PnO; Fig. 2G) and the reticulotegmental nucleus of the pons (RtTg; Fig 2G).

Within the medulla, labeling was detected in the prepositus nucleus (Pr; Fig. 2H), in the gigantocellular reticular nucleus (GI; Fig. 2H) and in the medial (MVe) and lateral vestibular nuclei (LVe; Fig. 2H). Furthermore, the dorsal motor nucleus of the vagus (DMV) showed strong PRCP mRNA and X-gal staining, together with the nucleus of solitary tract (NTS) and the nucleus ambiguous (Amb; Fig. 1H,R, Fig. 2I, Fig. 3L). Also in the medulla labeling was found in the spinal trigeminal nucleus (Sp5).

Furthermore, labeling was observed in the medullary reticular formation and in the cuneate and external cuneate nucleus (ECu; Fig. 2I).

Inconsistent or no signal was detected in the cerebellum (Fig. 2H).

3. Discussion

The generation of a transgenic mouse model, in which a specific cassette fused with LacZ reporter gene was inserted into PRCP gene, has allowed us to study via the X-gal staining the expression of PRCP throughout the CNS. In addition, to further confirm PRCP distribution, radioactive in situ hybridization using a riboprobe specific for PRCP mRNA was performed. Our study shows that PRCP is not only expressed in the hypothalamic region as previously reported (Wallingford et al., 2009; Jeong et al., 2012a, 2013) but in many other regions of the CNS. Several extra-hypothalamic areas showed considerable

PRCP expression, including the hippocampus, cortex, amygdala and several nuclei of the brain stem. The pattern of X-gal staining overall overlapped with that of the in situ hybridization. However, few discrepancies between the transgene and the endogenous PRCP mRNA expression in the brain were observed. For example, X-gal staining was negative and/or inconsistent in theVMH, the anterior hypothalamic area (AHA) and the BST, while a detectable level of silver grains was found in these areas. A possible explanation is that although PRCP mRNA is expressed in these areas, protein levels may not be detectable due to region-specific translational regulation. In addition, studies have suggested several possibilities for differential pattern between a transgene and the endogenous mRNA expression, including copy number, site of transgene fusion and size of transgene construct (Liu et al., 2003; Young et al., 1998; Daniel et al., 2005).

To date, the known substrates for PRCP are angiotensin II and III, prekallikrein and α-MSH. We have previously shown that PRCP is the enzyme responsible for the degradation of α-MSH (Wallingford et al., 2009) thus, it is a modulator of the melanocortin receptor signals. In accordance with that, PRCP is expressed in many hypothalamic and extra hypothalamic areas where melanocortin receptors 3 and 4 (MC3R and MC4R, respectively) expressions have been reported (Roselli-Rehfuss et al., 1993; Gantz et al., 1993; Liu et al., 2003; Daniel et al., 2005). For example, within the hypothalamus stronger expression was detected in the PVN, DMH and LH. All of these are known sites of MC4R expression. In addition, low expression has been detected in the ARCwhere POMC neurons are localized. Indeed, there is limited expression of MC3R in subpopulation of arcuate POMC and NPY/AgRP neurons (Jegou et al., 2000; Bagnol et al., 1999; Mounnien et al., 2005). In addition to hypothalamic nuclei, we found a considerably strong expression of PRCP also in the DMV and in the NTS. Both these brain stem areas express high levels of MC4R (Liu et al., 2003; Daniel et al., 2005), thus, suggesting that PRCP may also regulate melanocortin signaling in the brain stem. Intriguingly, a recent study showed that increased electrical activity of DMV neurons is associated with lower melanocortin tone (Sohn et al., 2013). These results support the finding that transgenic PRCP knockdown mice (*PRCP*$^{gt/gt}$ mice) are hypertensive (Adams et al., 2011). A decreased PRCP activity in this brain stem site, by increasing melanocortin signaling, may reduce the activity of DMV neurons, and therefore, the parasympathetic tone. This, in turn, could result in a relative increase of the sympathetic tone. In support of this, *PRCP*$^{gt/gt}$ mice have increased UCP1 mRNA levels (Jeong et al., 2012b), indication of an increased sympathetic activity, and do not show changes in the angiotensin/bradykinin system (Adams et al., 2011) suggesting the possible role of central PRCP in the cardiovascular phenotype of these mice.

Strong PRCP labeling was also detected in multiple limbic regions, including the hippocampus, lateral septal nucleus and amygdala where MC4R has been shown to be expressed (Liu et al., 2003; Daniel et al., 2005). PRCP has been also detected in the medial preoptic area, the medial habenular nucleus and the piriform cortex, sites expressing MC3R (Roselli-Rehfuss et al., 1993; Gantz et al., 1993).

Because of its ability to process virtually all small peptides with a proline as penultime amino acid, many more substrates for PRCP may exist. Our study showing the expression pattern of PRCP in the CNS could help to identify other substrates according to the area of PRCP expression.

4. Experimental Procedure

4.1 Animal

Young adult male C57Bl6 mice (3-5 months old) and PRCP gene trap (PRCP$^{gt/gt}$; 3-5 months old males) mice expressing LacZ reporter gene crossed for 10 generations to a

C57Bl6 (Wallingford et al., 2009; Jeong et al., 2012a, b, 2013) were used to determine endogenous PRCP mRNA and LacZ expression in the brain, respectively. Within each experimental group, mice with similar body weight were used. Animals were housed at Yale University animal facility under 12h light/ 12h dark cycle and a temperature at 25°C, and had a free access to standard chow diet (Harlan Teklad#2018). All of the studies were approved by Yale University Institutional Animal Care and Use Committee.

4.2 Radioactive in situ hybridization

Male mice (WT; n = 4) were sacrificed under deep anesthesia (Isothesia; Butler Schein Animal Health, Dublin, OH) and the brains were quickly removed and frozen in liquid nitrogen, and stored at −80°C until use. Coronal sections (20 μm) were cut throughout the brain using a cryostat (Leica's CM 1850, Wetzlar, Germany), mounted on slides, and stored at −80°C until use. Brain sections with a 200 μm interval (about 42 sections in 14 slides per each brain) were used for in situ hybridization. In situ hybridization using S^{35}-labeled riboprobes specific to PRCP was performed as previously reported (Jeong et al., 2012b, Jeong et al., 2013), with a hybridization temperature of 60°C for overnight. A sense riboprobe was used as control. The sense probe showed no hybridization signals throughout the brain. Emulsion autoradiography was performed after phosphorimager screening exposure (STORM 860 II phosphorimager, GE Health Care, USA). Data analysis was performed unbiased using a NIH Image J program, and a density of signal is represented by density per area.

4.3 X-gal staining

Mice ($PRCP^{gt/gt}$; n = 4) were perfused with 4% paraformaldehyde under anesthesia (Isothesia; Butler Schein Animal Health, Dublin, OH), and coronal sections (40 μm) were obtained with the use of a vibratome. Brain sections with a 120 μm interval were used for each brain for staining and analysis. X-gal staining was performed as previously reported (Wallingford et al., 2009). Briefly, sections were washed with PBS (137 mM NaCl, 2.7 mM KCl, 8 mM Na_2HPO_4, 2.6 mM KH_2PO_4) 4 times. Sections were then rinsed quickly once in cold PBS with 2 mM $MgCl_2$ and incubated in the above solution for 10 min at 4°C. Permeabilization was performed by incubation in cold PBS with detergent (0.01% sodium desoxycholate and 0.02% NP40) for 10 min. Sections were then incubated overnight at 37°C in the staining solution containing 25 mM $K_3Fe(CN)_6$, 25 mM $K_4Fe(CN)_63H2O$, 2 mM $MgCl_2$ in PBS and 1mg/ml of X-Gal. Sections were then rinsed in PBS, mounted on slides and analyzed unbiased under the microscope.

Acknowledgments

This work was supported by NIH grants DK 084065 (to S.D.)

Abbreviation

PRCP: CNS	Central Nervous System; Prolyl carboxypeptidase
α-MSH	alpha-melanocyte stimulating hormone
MC3R	melanocortin 3 receptor
MC4R	melanocortin 4 receptor
Lv	lateral ventricle
3v	third ventricle
4v	fourth ventricle

HP	hippocampus
HYP	hypothalamus
Thal	Thalamus
Amyg	amygdala
Cb	cerebellum
Cing Ctx	cingulate cortex
VTA	ventral tegmental area
NTS	nucleus of solitarius tract
DMV	dorsal motor nucleus of the vagus
f	fornix
ec	external capsule
Pir ctx	piriform cortex
ac	anterior commissure
MPO	medial preoptic nucleus
LPO	lateral preoptic area
PVN	paraventricular nucleus of hypothalamus
ARC	arcuate nucleus of the hypothalamus
VMH	ventromedial nucleus of the hypothalamus
DMH	dorsomedial hypothalamic nucleus
LH	lateral hypothalamus
SN	substantia nigra
BLA	basolateral amygdala
DG	dentate gyrus
Pir Ctx	piriform cortex
MPO	medial preoptic area
LPO	lateral preoptic area
LSN	lateral septal nucleus
SO	supraoptic nucleus
PV	paraventricular nucleus of the thalamus
Xi	xiphoid thalamic nucleus
MHb	medial habenular nucleus
VM	ventromedial nucleus of the thalamus
D3v	dorsal third ventricle
SN	substantia nigra
ZI	zona incerta
MM	mammillary body

VTA	ventrotegmental area
CA	cerebral aqueduct
Pn	pontine nuclei
PnO	pontine reticular nucleus
RtTg	reticulotegmental nucleus of the pons
LVe	lateral vestibular nucleus
MVe	medial vestibular nucleus
Pr	prepositus nucleus
Sp5	spinal trigeminal nucleus
Gi	gigantocellular reticular nucleus
ECu	external cuneate nucleus

References

Abeywickrema PD, Patel SB, Byrne NJ, Diehl RE, Hall DL, Ford RE, Rickert KW, Reid JC, Shipman JM, Geissler WM, Pryor KD, SinhaRoy R, Soisson SM, Lumb KJ, Sharma S. Expression, purification and crystallization of human prolylcarboxypeptidase. Acta crystallographica. Section F, Structural biology and crystallization communications. 2010; 66:702–705.

Adams GN, LaRusch GA, Stavrou E, Zhou Y, Nieman MT, Jacobs GH, Cui Y, Lu Y, Jain MK, Mahdi F, Shariat-Madar Z, Okada Y, D'Alecy LG, Schmaier AH. Murine prolylcarboxypeptidase depletion induces vascular dysfunction with hypertension and faster arterial thrombosis. Blood. 2011; 117:3929–3937. [PubMed: 21297000]

Bagnol D, Lu XY, Kaelin CB, Day HE, Ollmann M, Gantz I, Akil H, Barsh GS, Watson SJ. Anatomy of an endogenous antagonist: relationship between Agouti-related protein and proopiomelanocortin in brain. J Neuroscience. 1999; 19:RC26.

Daniel PB, Fernando C, Wu CSJ, Marnane R, Broadhurst R, Mountjoy KG. 1 kb of 5’ flanking seguence from mouse MC4R gene is sufficient for tissue specific expression in a transgenic mouse. Mol Cell Endocrinol. 2005; 239:63–71. [PubMed: 15950372]

Gantz I, Miwa H, Konda Y, Shimoto Y, Tashiro T, Watson SJ, DelValle J, Yamada T. Molecular cloning, expression, and gene localization of a fourth melanocortin receptor. J Biol Chem. 1993; 268:15174–15179. [PubMed: 8392067]

Jackman HL, Tan FL, Tamei H, Beurling-Harbury C, Li XY, Skidgel RA, Erdos EG. A peptidase in human platelets that deamidates tachykinins: Probable identity with the Iysosomal “protective protein.”. J Biol Chem. 1990; 265:13 265–11272. [PubMed: 2378615]

Jackman HL, Tan F, Schraufnagel D, Dragovic T, Dezso B, Becker RP, Erdos EG. Plasma membrane-bound and lysosomal peptidases in human alveolar macrophages. Am J Respir Cell Mol Biol. 1995; 13:1 96–204. [PubMed: 7598934]

Jegou S, Boutelet I, Vaudry H. Melanocortin-3 receptor mRNA expression in proopiomelanocortin neurons of the rat arcuate nucleus. J Neuroendocrinol. 2000; 12:501–505. [PubMed: 10844578]

Jeong JK, Szabo G, Raso GM, Meli R, Diano S. Deletion of prolyl carboxypeptidase attenuates the metabolic effects of diet-induced obesity. Am J Physiol Endocrinol Metab. 2012a; 302:E1502–1510. [PubMed: 22454290]

Jeong JK, Szabo G, Kelly K, Diano S. Prolyl carboxypeptidase regulates energy expenditure and the thyroid axis. Endocrinology. 2012b; 153:683–689. [PubMed: 22202165]

Jeong JK, Kim JD, Diano S. Ghrelin regulates hypothalamic prolyl carboxypeptidase expression in male mice. Molecular Metabolism. 2013; 2:23–30. [PubMed: 24024131]

Kumamoto K, Stewart TA, Johnson AR, Erdos EG. Prolylcarboxypeptidase (angiotensinase C) in human cultured cells. J Clin Invest. 1981; 67:210–215. [PubMed: 7451650]

Liu H, Kishi T, Roseberry AG, Cai X, Lee CE, Montez JM, Friedman JM, Elmquist JK. Transgenic mice expressing green fluorescent protein under the control of the melanocortin-4 receptor promoter. J Neurosci. 2003; 23:7143–7154. [PubMed: 12904474]

Miller JJ, Changaris DG, Levy RS. Angiorensin carboxypeptidase activity in urine from normal subjects and patients with kidney damage. Life Sci. 1991; 48:1529–1535. [PubMed: 2016986]

Mounien L, Bizet P, Boutelet I Vaudry H, Jegou S. Expression of melanocortin MC3 and MC4 receptor mRNAs by neuropeptide Y neurons in the rat arcuate nucleus. Neuroendocrinology. 2005; 82:164–170. [PubMed: 16508337]

Odya CE, Marinkovic DV, Hammon KJ, Stewart TA, Erdos EG. Purification and properties of prolylcarboxypeptidase (Angiotensinase C) from human kidney. J. Biol. Chem. 1978; 253:5927–5931. [PubMed: 28321]

Roselli-Rehfuss L, Mountjoy KG, Robbins LS, Mortrud MT, Low MJ, Tatro JB, Entwistle ML, Simerly RB, Cone RD. Identification of a receptor for gamma melanocortin and other proopiomelanocortin peptides in the hypothalamus and limbic system. Proc Natl Acad Sci. 1993; 90:8856–8860. [PubMed: 8415620]

Soisson SM, Patel SB, Abeywickrema PD, Byrne NJ, Diehl RE, Hall DL, Ford RE, Reid JC, Rickert KW, Shipman JM, Sharma S, Lumb KJ. Structural definition and substrate specificity of the S28 protease family: the crystal structure of human prolylcarboxypeptidase. BMC structural biology. 2010; 10:16. [PubMed: 20540760]

Skarners WC, Moss JE, Hurtley SM, Beddington RSP. Capturing genes encoding membrane and secreted proteins important for mouse development. Proc Natl Acad Sci. 1995; 92:6592–6596. [PubMed: 7604039]

Skidgel RA, Wickstrom F, Kumamoto K, Erdos EG. Rapid radioassay for prolylcarboxypeptidase (angiotensinase C). Anal Biochem. 1981; 118:113–119. [PubMed: 7337205]

Sohn JW, Harris LE, Berglund ED, Liu T, Vong L, Lowell BB, Balthasar N, Williams KW, Elmquist JK. Melanocortin 4 receptors reciprocally regulate sympathetic and parasympathetic preganglionic neurons. Cell. 2013; 152:612–619. [PubMed: 23374353]

Tan F, Morris PW, Skidgel RA, Erdos EG. Sequencing and cloning of human prolylcarboxypeptidase (angiotensinase C). Similarity to both serine carboxypeptidase and prolylendopeptidase families. J Biol Chem. 1993; 268(22):16631–8. [PubMed: 8344943]

Wallingford N, Perroud B, Gao Q, Coppola A, Gyengesi E, Lui ZW, Gao XB, Diament A, Haus KA, Shariat-Madar Z, Mahdi F, Wardlaw SL, Schmaier AH, Warden CH, Diano S. Prolylcarboxypeptidase regulates food intake by inactivating -MSH in rodents. J Clin Invest. 2009; 119:2291–2303. [PubMed: 19620781]

Yang HYT, Erdos EG, Chiang TS. New enzymatic route for the inactivation of angiotensin. Nature. 1968; 218:1224–1226. [PubMed: 4297812]

Yang HYT, Erdos EG, Chiang TS, Jenssen TA, Rodgers JG. Characteristics of an enzyme that inactivates angiotensin II (angiotensinase C). Biochem Pharmacol. 1970; 19:1201–1211.

Young JI, Otero V, Cerdan MG, Falzone TL, Chan EC, Low MJ, Rubinstein M. Authentic cell-specific and developmentally regulated expression of pro-opiomelanocortin genomic fragments in hypothalamic and hindbrain neurons of transgenic mice. J Neurosci. 1998; 18:6631–6640. [PubMed: 9712635]

Highlights

1. Wide expression of Prolyl carboxypeptidase (PRCP) in the Central Nervous System (CNS)
2. PRCP expression pattern overlaps with that of melanocortin receptors
3. Additional PRCP substrates and roles may be identified from its CNS distribution

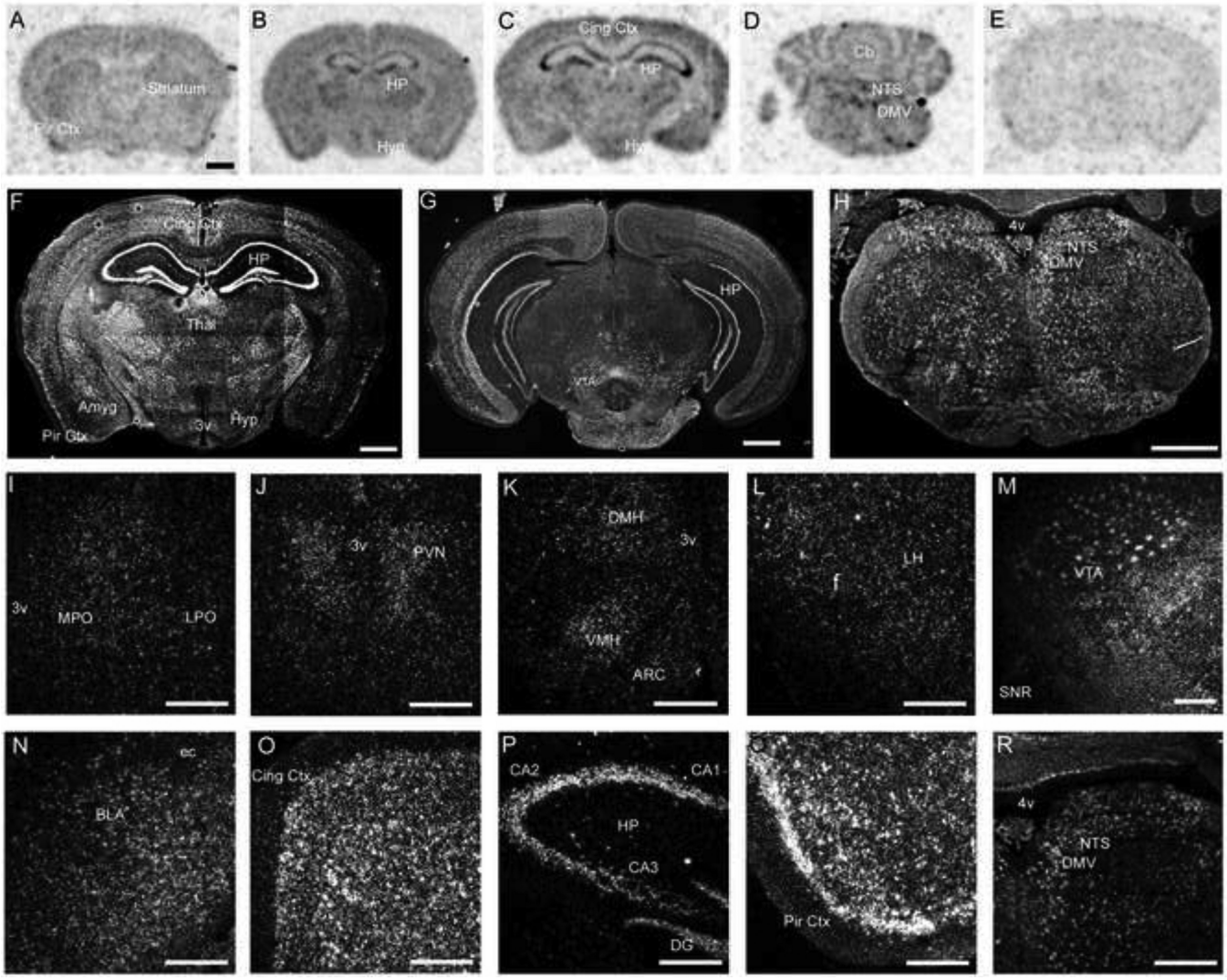

Fig. 1.

Representative images of coronal sections of mouse brain showing PRCP mRNA expression by radioactive in situ hybridization. Panels A-D; Brain coronal section images obtained from phosphorimager showing the overall brain expression patter of PRCP mRNA from rostral to caudal extent. Panel E shows signal from sense riboprobes as a negative control. Panels F-H: darkfield picture collage of representative coronal sections of mouse brain showing hybridization signals (silver grains) for PRCP mRNA. Panels I-R: darkfield high power magnification micrographs showing hybridization signals (silver grains) for PRCP mRNA in of several brain areas. Abbreviation: 3v: third ventricle; 4v: fourth ventricle; HP: hippocampus; HYP: hypothalamus; Thal: Thalamus; Amyg: amygdala; Cb: cerebellum; Cing Ctx: cingulate cortex; VTA: ventral tegmental area; NTS: nucleus of solitarius tract; DMV: dorsal motor nucleus of the vagus; f: fornix; ec: external capsule; Pir ctx: piriform cortex; ac: anterior commissure; MPO: medial preoptic nucleus; LPO: lateral preoptic area; PVN: paraventricular nucleus of hypothalamus; ARC: arcuate nucleus of the hypothalamus; VMH: ventromedial nucleus of the hypothalamus; DMH: dorsomedial hypothalamic nucleus; LH: lateral hypothalamus; SNR: substantia nigra reticulate; BLA: basolateral amygdala; DG: dentate gyrus. Scale bar in A (for A-E) represents 1 mm. Bar scales in F-H represent 1 mm; Bar scales in I-R represent 200 μm.

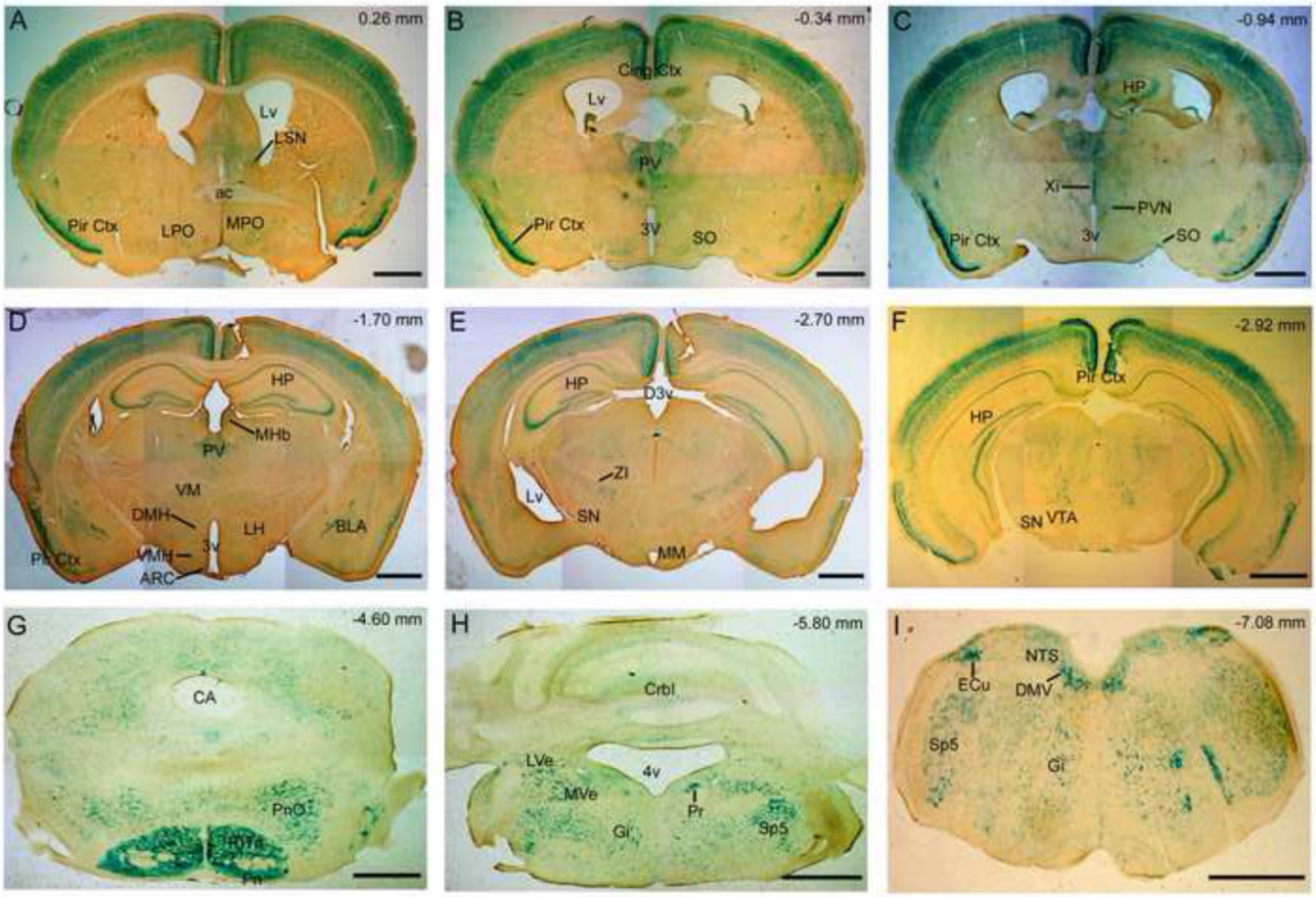

Fig 2.

Picture collage of representative coronal sections of *PRCP*$^{gt/gt}$ mouse brain showing the distribution of LacZ (X-gal staining). Abbreviations: Pir Ctx: piriform cortex; MPO: medial preoptic area; LPO: lateral preoptic area; Lv: lateral ventricle; LSN: lateral septal nucleus; 3v: third ventricle; Cing Ctx: cingulate cortex; SO: supraoptic nucleus; PV: paraventricular nucleus of the thalamus; HP: hippocampus; Xi: xiphoid thalamic nucleus; PVN: paraventricular nucleus of the hypothalamus; MHb: medial habenular nucleus; VM: ventromedial nucleus of the thalamus; DMH: dorsamedial nucleus of the hypothalamus; VMH: ventromedial nucleus of the hypothalamus; ARC: arcuate nucleus of the hypothalamus; BLA: basolateral amygdala; D3v: dorsal third ventricle; SN: substantia nigra; ZI: zona incerta; MM: mammillary body; VTA: ventrotegmental area; CA: cerebral aqueduct; Pn: pontine nuclei; PnO: pontine reticular nucleus; RtTg: reticulotegmental nucleus of the pons; Cb: cerebellum; 4v: fourth ventricle; LVe: lateral vestibular nucleus; MVe: medial vestibular nucleus; Pr: prepositus nucleus; Sp5: spinal trigeminal nucleus; Gi: gigantocellular reticular nucleus; NTS: nucleus of the solitarius tract; DMV: dorsal motor nucleus of the vagus; ECu: external cuneate nucleus. All scale bars represent 1mm.

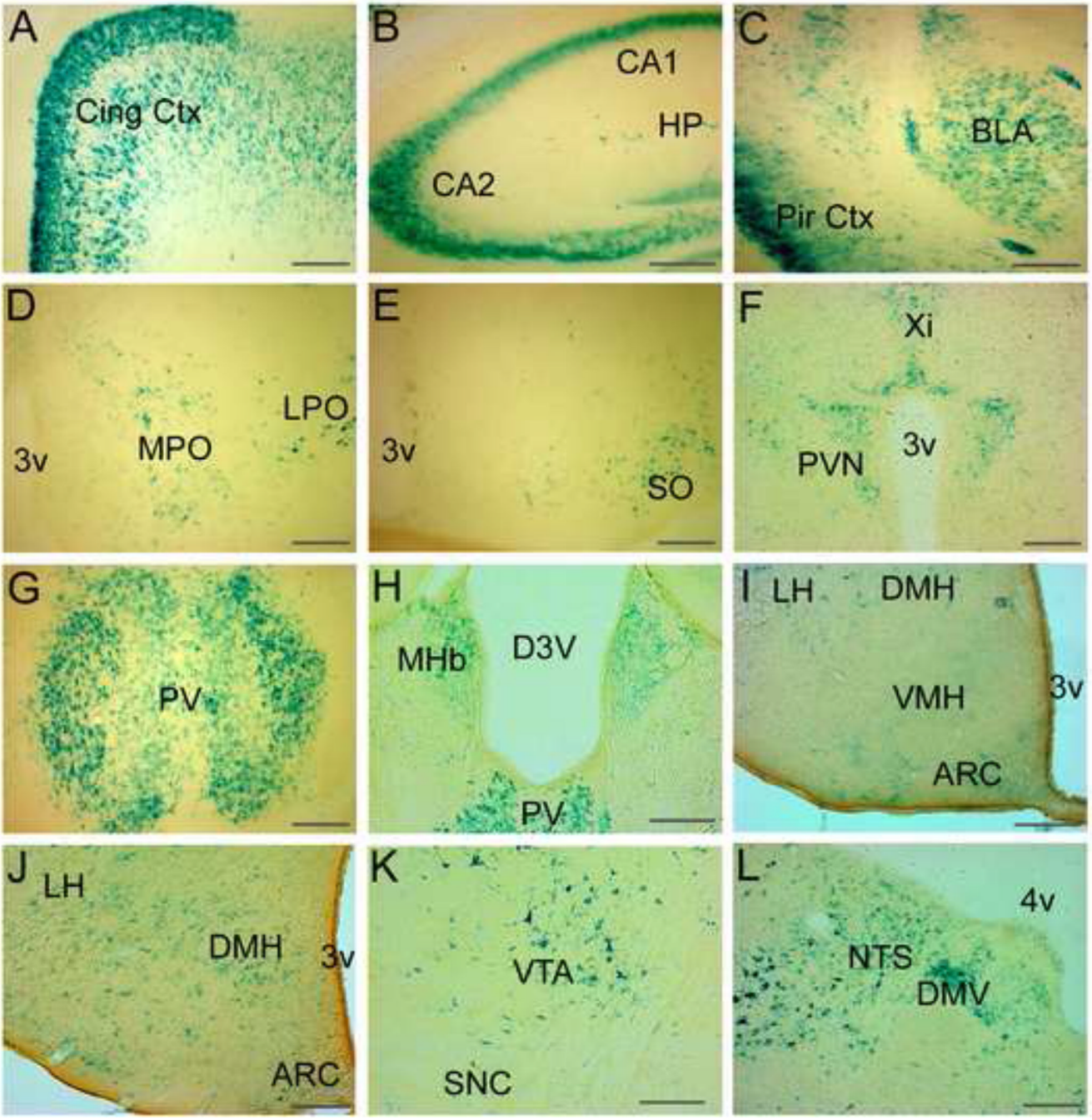

Fig. 3.

Representative high power micrographs showing LacZ expression in *PRCP*$^{gt/gt}$ mouse brain in various brain regions. Panel A: cingulate cortex (Cing Ctx). Panel B: hippocampal (HP) regions Ca1 and CA2; Panel C: piriform cortex (Pir Ctx) and basolateral amygdala (BLA). Panel D: medial (MPO) and lateral preopotic area (LPO). Panel E: supraoptic nucleus (SO). Panel F: Xiphoid thalamic nucleus (Xi) and paraventricular nucleus of the hypothalamus (PVN). Panel G: paraventricular nucleus of the thalamus (PV). Panel H: paraventricular nucleus of the thalamus (PV) and medial habenular nucleus (MHb). Panel I: dorsomedial (DMH), ventromedial (VMH) and arcuate nucleus of the hypothalamus (ARC). Panel J: lateral hypothalamus (LH) and dorsomedial nucleus of the hypothalamus (DMH). Panel K:

ventral tegmental area (VTA) and substantia nigra (SN). Panel L: nucleus of the solitarius tract (NTS) and dorsal motor nucleus of the vagus (DMV). All scale bars represent 100 μm.

Table 1

PRCP transgene and endogenous PRCP mRNA expression in the mouse brain

Telencephalon:		
Hippocampus	LacZ	PRCP mRNA
Dentate Gyrus (DG)	+++	+++
Ammon's horn, CA 1	++++	++++
Ammon's horn CA 2	+++++	+++++
Ammon's horn CA 3	++++	++++
Amygdaloid		
Basolateral amygdaloid nucleus, anterior part (BLA)	+++	+++
Basolateral amygdaloid nucleus, ventral part (BLV)	+++	+++
Anterior amygdaloid area, ventral part (AAV)	++	++
Central amygdaloid nuclei	+++	+++
Septum pellucidum		
Lateral septal nucleus (LSN)	++	++
Cerebral cortex		
Retrosplenial granular (RSG)	+++++	+++++
Retrosplenial agranular cortex (RSA)	+++++	+++++
Piriform cortex (Pir Ctx)	+++++	+++++
Other areas of the cortex	+++	+++
Diencephalon:		
Hypothalamus		
Lateral preoptic area (LPO)	++	++
Medial preoptic area (MPO)	+/−	++
Paraventricular nucleus (PVN)	++/+++	++/+++
Supraoptic nucleus (SO)	++	++
Lateral hypothalamus (LH)	++	++
Ventromedial hypothalamus (VMH)	+/−	++
Arcuate nucleus (ARC)	+	+
Dorsomedial hypothalamus (DMH)	++	++
Anterior hypothalamic area (AH)	+	+
Premammillary nucleus, ventral part (PMV)	+	+
Premammillary nucleus, dorsal part (PMD)	+	+
Thalamus		
Xiphoid thalamic nucleus (Xi)	+++	+++
Central medial thalamic nucleus (CM)	+	+
Ventromedial (VM)	++	++
Zona incerta, ventral part (ZIV)	++	++
Intermediodorsal thalamic nucleus (IMD)	++	++
Bed nucleus of stria terminalis (BST)	+/−	++
Ethmoid thalamic nucleus (Eth)	++	++
Paraventricular thalamic nucleus (PV)	++++	++++

Epithalamus		
Habenular nucleus	++	++
Mesencephalon, Metencephalon and Myelencephalon:		
Ventral tegmental area (VTA)	++/+++	++/+++
Substantia nigra, reticular part (SNR)	+/−	+/++
Reticulotegmental nucleus of the pons (RtTg)	++++	++++
Locus coeruleus (LC)	++	++
Motor trigeminal nucleus (Mo 5)	+++	+++
Principal sensory trigeminal nucleus (Pr5)	++	++
Pontine reticular nucleus, caudal part (PnC)	++	++
Pontine reticular nucleus, oral part (PnO)	+/−	+
Medullary reticular nucleus, dorsal part (MdD)	++	++
Medullary reticular nucleus, ventral part (MdV)	++	++
Intermediate reticular nucleus (IRt)	++	++
Lateral reticular nucleus (LRt)	++	++
Gigantocellular reticular nucleus (Gi)	++	++
Nucleus of trapezoid body (Tz)	+/++	+/++
Lateral vestibular nucleus (LVe)	++	++
Parvicellular reticular nucleus, alpha part (PCRtA)	++	++
Spinal trigeminal nucleus, (SP5)	++	++
Nucleus of solitary tract (NTS)	++	++
Dorsal motor of vagus (DMV)	+++	+++
Prepositus nucleus (Pr)	+	+
Medial vestibular nucleus, parvicellular part (MVePC)	+	+
Cuneate nucleus (Cu)	+++	+++
External cuneate nucleus (ECu)	++++	++++